

# Boundedness of solutions of a non-local reaction–diffusion model for adhesion in cell aggregation and cancer invasion

JONATHAN A. SHERRATT<sup>1</sup>, STEPHEN A. GOURLEY<sup>2</sup>,  
NICOLA J. ARMSTRONG<sup>1</sup> and KEVIN J. PAINTER<sup>1</sup>

<sup>1</sup>*Department of Mathematics and Maxwell Institute for Mathematical Sciences,  
Heriot-Watt University, Edinburgh EH14 4AS, UK*

<sup>2</sup>*Department of Mathematics, University of Surrey, Guildford, Surrey GU2 7XH, UK  
email: jas@ma.hw.ac.uk, S.Gourley@surrey.ac.uk  
nicola\_j\_armstrong@hotmail.com, painter@ma.hw.ac.uk*

(Received 14 December 2007; revised 4 September 2008; first published online 19 November 2008)

Adhesion of cells to one another and their environment is an important regulator of many biological processes but has proved difficult to incorporate into continuum mathematical models. This paper develops further the new modelling approach proposed by Armstrong *et al.* (A continuum approach to modelling cell–cell adhesion, *J. Theor. Biol.* 243: 98–113, 2006). The models studied in the present paper use an integro-partial differential equation for cell behaviour, in which the integral represents the sensing by cells of their local environment. This enables an effective representation of cell–cell adhesion, as well as random cell movement, and cell proliferation. The authors use this modelling approach to investigate the ability of cell–cell adhesion to generate spatial patterns during cell aggregation. The model is also extended to give a new representation of cancer growth, whose solutions reflect the balance between cell–cell and cell–matrix adhesion in regulating cancer invasion. The non-local term in these models means that there is no standard theory from which one can deduce the boundedness required for biological realism: specifically, solutions for cell density must lie between zero and a positive density corresponding to close cell packing. Here the authors derive a number of conditions, each of which is sufficient for the required boundedness, and they demonstrate numerically that cell density increases above the upper bound for some parameter sets not satisfying these conditions. Finally the authors outline what they regard as the main mathematical challenges for future work on boundedness in models of this type.

## 1 Introduction

Most biological cells adhere to one another and to their environment via adhesion molecules on their surface. This is an important regulator of many aspects of physiology and pathology; for example, adhesion plays a key role in the early stages of vertebrate development (Cheng *et al.*, 2005; Halbleib & Nelson, 2006) and is central to the invasive stage of cancer (Gassmann *et al.*, 2004; Hart, 2005). For recent general reviews of cell adhesion, see Foty and Steinberg (2005), Reddig and Juliano (2005) and Steinberg (2007).

Theoretical study of cell adhesion has a relatively long history of using computational individual cell-based models. Key early work of this type was done by Glazier and co-workers (Graner & Glazier, 1992; Glazier & Graner, 1993; Glazier *et al.*, 1995; Mombach *et al.*, 1995), who adapted the Potts model from theoretical physics to biological cell populations. Here each cell is composed of a number of sites on a fixed grid, and sites change cell type according to an energy minimisation scheme that depends on contacts between neighbouring cells. This approach has been extended and refined by a number of authors, with applications to cellular slime mould morphogenesis (Savill & Hogeweg, 1997; Maree & Hogeweg, 2002), vertebrate development (Zajac *et al.*, 2000; Merks & Glazier, 2005), epidermal homeostasis (Savill & Sherratt, 2003) and solid tumour growth (Stott *et al.*, 1999; Turner *et al.*, 2004; Bauer *et al.*, 2007). Other lattice-based models incorporating cell adhesion include work of Grygierzec *et al.* (2004) and Anderson *et al.* (2006) on solid tumour growth, and the model of Moreira and Deutsch (2005) for pigmentation patterning in zebrafish. Recent reviews of lattice-based models are given in the books by Deutsch and Dormann (2005; Chapter 7 focusses on cellular adhesion) and Anderson *et al.* (2007, Sections I and II).

A different type of individual cell-based model is of 'lattice free' type, in which cells are tracked as they move through continuous space. Work of this type includes two important series of papers, by Othmer and co-workers and by Drasdo and co-workers. The former involves a detailed representation of the mechanical forces, including adhesive forces, that underlie cell movement; applications have mainly been focussed on cellular slime moulds (Palsson & Othmer, 2000; Dallon & Othmer, 2004; Palsson, 2007), although a recent paper concerns avascular tumour growth (Kim *et al.*, 2007). A similar approach has recently been used to study cohesive and adhesive effects during platelet aggregation in blood clotting (Fogelson, 2007; Fogelson & Guy, 2008).

The approach of Drasdo and co-workers uses a similar framework, but with a focus on cell population dynamics rather than mechanical forces; applications have been to tumour growth (Drasdo *et al.*, 1995; Drasdo & Hohme, 2003, 2005), epidermal homeostasis (Galle *et al.*, 2005; Schaller & Meyer-Hermann, 2007) and early development (Drasdo & Forgacs, 2000; Drasdo & Loeffler, 2001). Recent reviews of lattice-free individual cell-based models are given by Galle *et al.* (2006) and in Sections III and IV of the book by Anderson *et al.* (2007).

It is relatively straightforward to include adhesive effects in individual cell-based models because they include explicit representations of the cell boundaries. However, there is no corresponding way to incorporate cell adhesion in continuous mathematical models for cellular dynamics. This is because adhesion is intrinsically a non-local phenomenon; a natural comparison is with cell movement up chemical gradients ('chemotaxis'), which can be effectively modelled as a local process (see Hillen & Painter (2008) for a recent review). Therefore the extensive literature on PDE models of cell movement mostly neglects adhesive effects. The main exception is a class of models that incorporate adhesion via a surface tension on the tumour boundary (Byrne & Chaplain, 1996; Chaplain, 1996; Cristini *et al.*, 2003; Frieboes *et al.*, 2006, 2007; Friedman, 2007; Macklin & Lowengrub, 2007). Other isolated exceptions are the use by Perumpanani *et al.* (1996) of a non-linear diffusion term to reflect reduced cell movement in regions of high cell density and Byrne's (1997) approximation of cell-cell adhesion at the surface of a solid tumour by a variation

in nutrient uptake, which is assumed to correlate with the strength of adhesive bonds. In all of these cases, the representation of adhesion is indirect: there is no explicit modelling of cell–cell contact. Recently, three of us proposed a new model for cell adhesion which does have a direct representation of this kind (Armstrong *et al.*, 2006). The model is of integro-partial differential equation form, with the non-local term representing adhesion via an integral over the ‘sensing region’ of a cell. Numerical simulations of this model reproduce a number of basic properties of adhesive cell populations. Moreover, the model has been successfully applied to somite formation in early vertebrate development (Armstrong *et al.*, in press) and to solid tumour growth (Gerisch & Chaplain, 2008). Green *et al.* (in preparation) have also used a very similar modelling framework to study liver cell aggregation.

This paper concerns models for cell aggregation and cancer invasion, based on the approach of Armstrong *et al.* (2006). The non-local form of our models means that there is relatively little general theory from which its underlying mathematical properties can be determined. In particular, biological realism demands that solutions for cell density be bounded both below (by zero) and above (by a density corresponding to close cell packing). The key results of this paper are Propositions 1 and 2 in Section 4, which give a series of conditions that are sufficient for these boundedness requirements to hold. Before discussing these results, we describe the basic form of the mathematical model in Section 2 and then an extended model for cancer invasion in Section 3. Finally, in Section 5, we discuss open mathematical questions on the boundedness properties of models of this type.

## 2 The basic mathematical model

Our model for an adhesive cell population is based on the work of Armstrong *et al.* (2006). We consider an integro-advection-diffusion equation in which the integral represents the effect of adhesion between cells on their movement:

$$\frac{\partial n(x, t)}{\partial t} = \overbrace{D \frac{\partial^2 n(x, t)}{\partial x^2}}^{\text{Random movement}} - \underbrace{\frac{\alpha \phi}{R} \frac{\partial}{\partial x} \left[ n(x, t) \int_{-R}^R A(n(x + x_0, t)) \omega(x_0) dx_0 \right]}_{\text{Adhesion}} + \underbrace{f(n)}_{\text{Cell kinetics}}. \quad (1)$$

Here  $n(x, t)$  is the cell density at position  $x$  and time  $t$ .  $D$ ,  $\alpha$ ,  $\phi$  and  $R$  are positive constants, a full description of which can be found in Armstrong *et al.* (2006). In brief,  $D$  is the diffusion coefficient,  $\alpha$  is the adhesion coefficient,  $\phi$  relates to the viscosity of the cells and  $R$  describes the radius over which cells can sense their surroundings, via protrusions such as filopodia. These protrusions cause adhesive bonds to form between cells that are significantly separated, and it is the making and breaking of these adhesive bonds that generate an adhesive cell flux (see Lock *et al.* (2008) or Alberts *et al.* (2008, pp. 1133–1150) for a detailed discussion). The function  $A(n)$  represents the attractive adhesive force between the cells. This force will increase with cell density when this is small, but will decrease at higher cell densities as close-packing is approached, with  $A = 0$  at the cell density  $n = n_{\max}$  corresponding to close-packing. Values of  $n > n_{\max}$  are not

biologically meaningful, but it is mathematically convenient to set  $A(n) = 0$  for  $n > n_{\max}$ . Armstrong *et al.* (2006) take  $A(n) = \max\{n(1 - n/n_{\max}), 0\}$  as a simple function with an appropriate qualitative form.

The function  $\omega(\cdot)$  represents the variation in adhesive force over the sensing region of the cell; for uniqueness, we impose the condition  $\int_0^R \omega(x_0) dx_0 = 1$ . There is a natural constraint that  $\omega(\cdot)$  is odd, since adhesive forces will always be directed towards cell centres, but otherwise there is no data that we are aware of on which  $\omega(\cdot)$  can be based. Armstrong *et al.* (2006) take  $\omega(x_0) = (1/R) \text{sign}(x_0)$  (though with a different scaling factor) as their basic functional form for mathematical simplicity.

The function  $f(n)$  represents cell division and cell loss, and must satisfy  $f(0) = 0$ . Again, this function will increase with cell density when this is small, but will decrease due to crowding pressure at higher values of  $n$ . Cell division and death are subject to separate regulatory mechanisms (see Jorgensen & Tyers (2004) or Alberts *et al.* (2008, Chapters 17 and 18) for review), and there will be a critical value  $n = n_0$  above which cell loss occurs more rapidly than the generation of new cells via division, so that  $f(n) < 0$  for  $n > n_0$ . This shift in the balance between division and loss must occur at an achievable cell density, and thus  $n_0 < n_{\max}$ , the close-packing density, which is an upper bound on  $n$  for biologically realistic solutions.

In the remainder of this section, we fix the functional forms as  $A(n) = \max\{n(1 - n/n_{\max}), 0\}$ ,  $\omega(x_0) = (1/R) \text{sign}(x_0)$  and  $f(n) = \mu n(1 - n/n_0)$ . Equation (1) then has exactly the form studied by Armstrong *et al.* (2006), except for the addition of the cell proliferation term. For algebraic simplicity, we non-dimensionalise (1) using the following rescalings:

$$x^* = x/R, \quad t^* = tD/R^2, \quad n^* = 2n/n_{\max}, \quad \alpha^* = \alpha\phi n_{\max}/(4D), \quad \mu^* = \mu R^2/D, \quad n_0^* = 2n_0/n_{\max}.$$

Substituting these into (1) and dropping the asterisks gives the dimensionless equations

$$\frac{\partial n(x, t)}{\partial t} = \frac{\partial^2 n(x, t)}{\partial x^2} - \alpha \frac{\partial}{\partial x} \left[ n(x, t) \int_{-1}^1 \max\{n(x + x_0, t)[2 - n(x + x_0, t)], 0\} \text{sign}(x_0) dx_0 \right] + \mu n(1 - n/n_0). \quad (2)$$

Armstrong *et al.* (2006) showed that in the absence of proliferation ( $\mu = 0$ ), (2) predicts the aggregation of an initially uniform cell population (with a small amount of noise) into discrete cell clusters. Such aggregation is well documented in *in vitro* experiments (see for example Steinberg, 1962; Foty & Steinberg, 2004, 2005). The model (2) has a unique non-zero spatially uniform steady state  $n = n_0$ , and intuitively one expects aggregation patterns to be possible when this steady state is unstable. Straightforward linear stability analysis gives the dispersion relation

$$\lambda = -\gamma^2 + 4\alpha n_0(1 - n_0)(1 - \cos \gamma) - \mu$$

for the growth rate  $\lambda$  of perturbations of wavenumber  $\gamma$  to  $n = n_0 < 2$ . Therefore the condition for instability is

$$4\alpha n_0(1 - n_0) > \min_{\gamma > 0} \left( \frac{\gamma^2 + \mu}{1 - \cos \gamma} \right) = \frac{4\theta^2 + \mu}{2 \sin^2 \theta}, \quad (3)$$

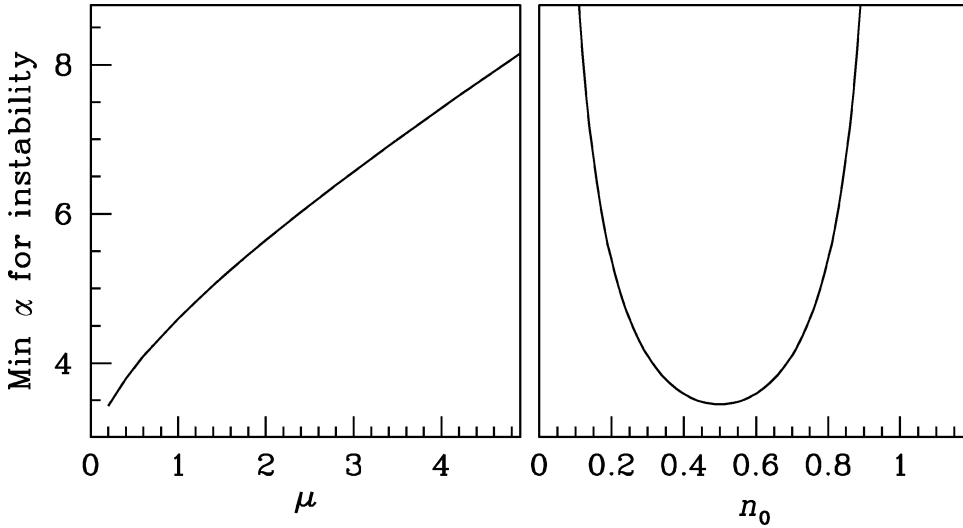


FIGURE 1. Illustrations of the condition (3) for stability of the uniform steady state  $n = n_0$  in the model (2) for cell aggregation. For given values of  $n_0$  and  $\mu$ , (3) defines a critical value of  $\alpha$  above which  $n = n_0$  is unstable. We plot this critical value of  $\alpha$  as a function of  $\mu$  for  $n_0 = 0.75$ , and as a function of  $n_0$  for  $\mu = 1$ . When the steady state is unstable, we expect intuitively that aggregation patterns will develop, and this is confirmed by numerical simulations (for example, Figure 2).

where  $\theta$  is the unique solution on  $(0, \pi/2)$  of  $\tan \theta = (4\theta^2 + \mu)/(4\theta)$ . This condition is illustrated in Figure 1. As the rate of cell turnover increases, higher levels of adhesion are required to generate aggregations. This prediction could be tested in experiments, but we are not aware of any relevant existing data. In Figure 2 we plot the results of numerical solutions of (2) for initial conditions in which a small amount of noise is added to the steady state  $n = n_0$ . These solutions confirm that the steady state is stable unless (3) is satisfied, in which case a pattern of cell aggregations develops.

### 3 Applications to cancer invasion

Cancer invasion is the process of cells migrating away from a solid tumour and into the surrounding extracellular matrix. It is a key early stage in metastasis: as they move through the matrix around the tumour, cells may encounter a blood vessel and be transported in the blood stream, potentially initiating a secondary tumour in a different part of the body. Cancers typically become invasive as a result of mutations affecting some combination of their production of enzymes that degrade extracellular matrix, their tendency to move up matrix gradients ('haptotaxis') and changes in their adhesiveness (reviewed by Hart (2005) and Ala-aho & Kähäri (2005)). The first two of these processes have been studied in a large number of mathematical models of both discrete and continuous (PDE) forms; see Araujo and McElwain (2004, Sections 4 and 6.4) and Chaplain & Lolas (2005, Section 2) for reviews. The role of cell–cell adhesion has received significant attention in discrete models (for example Turner & Sherratt (2002); Anderson (2005)). However, the lack of an effective modelling approach means that adhesion has been neglected in most continuum

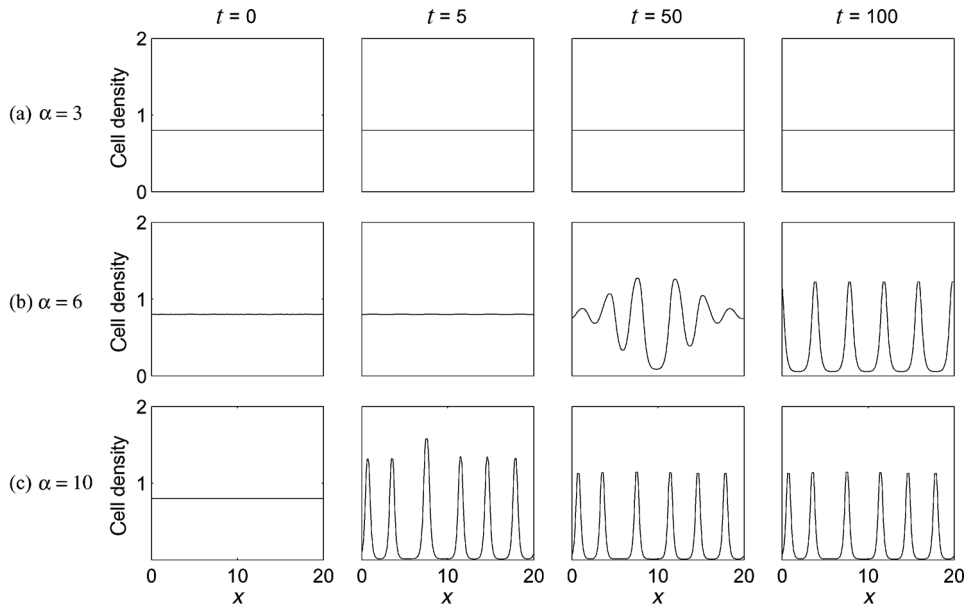


FIGURE 2. Numerical solutions of the model (2) with three different values of the adhesion strength parameter  $\alpha$ . At  $t=0$  we impose a small level of noise to  $n=n_0$ ; specifically  $n(x,0)=n_0+\Phi(x)$ , with  $\Phi(\cdot)$  chosen randomly at each grid point from a uniform distribution between  $\pm 5 \times 10^{-4}$ . We fix  $\mu=1$  and  $n_0=0.8$ , in which case (3) implies that the steady state  $n=n_0$  will be stable when  $\alpha < 5.38\dots$ . In (a) we take  $\alpha=3$  so that this condition is satisfied, and the solution returns to  $n \equiv n_0$ . In (b) and (c),  $\alpha=6$  and  $10$  respectively, and aggregation patterns develop. We use periodic boundary conditions, and the equations were solved numerically using a finite volume scheme with first-order upwinding. The resulting system of ODEs was solved using ROWMAP (Weiner *et al.*, 1997; see also Gerisch & Chaplain, 2008), a stiff integrator based on a Rosenbrock-type method. The spatial grid spacing was 0.1. A detailed discussion of methods for numerical evaluation of the integral term in equations such as (2) is given by Gerisch (submitted).

models of cancer invasion. The most successful previous approach has been to represent cell–cell adhesion as a surface tension on the tumour boundary (Byrne & Chaplain, 1996; Chaplain, 1996; Cristini *et al.*, 2003; Frieboes *et al.*, 2006, 2007; Macklin & Lowengrub, 2007). However, this does not allow an investigation of the role of cell–matrix adhesion, which also plays a key role in cancer invasion (see Berrier & Yamada (2007) for a review). The standard paradigm is that invasive cancer cells have decreased cell–cell adhesion and/or increased cell–matrix adhesion in comparison to their non-invasive counterparts (see Zigrino *et al.* (2005) for a detailed biological discussion). The modelling approach of Armstrong *et al.* (2006) provides a natural way of investigating how changes in cell–cell and cell–matrix adhesiveness can conspire to produce an invasive phenotype, and we now describe a simple model of this type.

The model is formulated in terms of the densities  $n(x,t)$  of tumour cells and  $m(x,t)$  of extracellular matrix; as in Section 2, we restrict attention to one space dimension for simplicity. We assume that cell movement is driven entirely by the adhesion of cells to one another and to the extracellular matrix. In reality, other factors such as chemical gradients make important contributions to cell movement, but we neglect these in order

to focus specifically on adhesion. It is natural to assume that cells have the same sensing radius for both types of adhesion, since both will be determined by the extension of cell protrusions such as filopodia. On the same basis we take the decrease in adhesive force with cell and matrix densities to be the same for both adhesion types; for simplicity, we assume a linear decrease. Our model equations are then

$$\begin{aligned}
 n_t &= \overbrace{k_1 n \left(1 - \frac{n}{k_2}\right)}^{\text{Proliferation}} \\
 &\quad - \overbrace{\left[ n \frac{\alpha \phi}{R} \int_{-R}^R n(x+x_0, t) \max \left\{ K - \frac{n(x+x_0, t)}{k_3} - \frac{m(x+x_0, t)}{k_4}, 0 \right\} \omega(x_0) dx_0 \right]_x}^{\text{Cell-cell adhesion}}, \\
 &\quad - \overbrace{\left[ n \frac{\beta \phi}{R} \int_{-R}^R m(x+x_0, t) \max \left\{ K - \frac{n(x+x_0, t)}{k_3} - \frac{m(x+x_0, t)}{k_4}, 0 \right\} \omega(x_0) dx_0 \right]_x}^{\text{Cell-matrix adhesion}} \quad (4a)
 \end{aligned}$$

$$m_t = \underbrace{-k_5 k_6 n m^2}_{\text{Proteolysis}}, \quad (4b)$$

where  $\alpha, \beta, \phi, R, K$  and the  $k_i$ 's are positive constants. The second equation represents the degradation of extracellular matrix by proteolytic enzymes. In many cases, these are produced by the tumour cells, in response to interactions with extracellular matrix (see Zigrino *et al.* (2005, Section 4) for a review of the relevant biological literature). A suitable equation for the concentration  $P(x, t)$  of enzyme would be  $P_t = k_7 n m - k_8 P$ , with  $m_t = -k_6 m P$  being the equation for matrix density. Proteolytic enzymes have very fast dynamics in comparison to those of cells and extracellular matrix, so that  $k_7$  and  $k_8$  are large in comparison to  $k_1$  and  $k_6$ . Therefore a quasi-steady-state assumption is appropriate, giving  $P = (k_7/k_8)nm$ , which implies (4b), with  $k_5 = k_7/k_8$ .

The parameters  $k_1$  and  $k_2$  reflect the dependence of cell division on local cell density, and  $K, k_3$  and  $k_4$  relate to the restrictions imposed by the availability of space on cellular sensing of the local environment. The parameters  $\phi$  and  $R$  and the function  $\omega_0$  have the same interpretation as in the model (1). For notational simplicity we non-dimensionalise the model using the rescalings

$$\begin{aligned}
 x^* &= \frac{x}{R}, \quad t^* = k_1 t, \quad n^* = \frac{2n}{k_3 K}, \quad m^* = \frac{2m}{k_4 K}, \\
 \alpha^* &= \frac{\alpha K^2 \phi k_3}{4k_1 R}, \quad \beta^* = \frac{\beta K^2 \phi k_4}{4k_1 R}, \quad \gamma = \frac{k_3 k_4 k_5 k_6 K^2}{4k_1}, \quad n_0 = \frac{2k_2}{k_3 K}, \quad \omega^*(\xi) = R\omega(\xi R).
 \end{aligned}$$

Substituting these into (4) and dropping the asterisks gives the dimensionless equations

$$\begin{aligned}
 n_t &= n(1 - n/n_0) - \frac{\partial}{\partial x} \left[ n \int_{-1}^1 [\alpha n(x+x_0, t) + \beta m(x+x_0, t)] \right. \\
 &\quad \left. \cdot \max \{2 - n(x+x_0, t) - m(x+x_0, t), 0\} \omega(x_0) dx_0 \right], \quad (5a)
 \end{aligned}$$

$$m_t = -\gamma n m^2. \quad (5b)$$

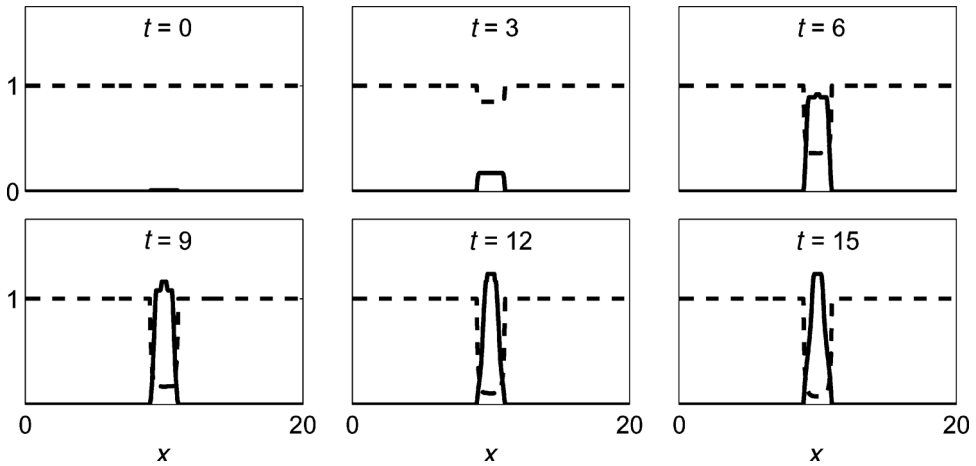


FIGURE 3. Numerical simulation of non-invasive tumour growth using the model (5). Initially we introduce a small population of tumour cells into a uniform level of extracellular matrix; specifically  $n=0.01$  on  $9 < x < 11$  and zero elsewhere, and  $m \equiv 1$ , at  $t=0$ . The parameter values  $\alpha=1$ ,  $\beta=0.8$ ,  $\gamma=1$  and  $n_0=1$  are such that the tumour population grows but does not invade the surrounding matrix. The function  $\omega(x_0)=\text{sign}(x_0)$ , and the equations were solved numerically as described in the legend to Figure 2. A detailed discussion of methods for numerical evaluation of the integral term in equations such as (5) is given by Gerisch (submitted). The boundary conditions were zero flux. For the integral, these are implemented by assuming that there are no cells located outside the domain. Since the adhesion term only allows cells to move to regions with positive cell density, this prevents movement over the boundary. Note however that the cell density remains almost zero close to the boundary.

The four dimensionless parameters have simple biological interpretations.  $\alpha$  and  $\beta$  reflect the strengths of cell–cell and cell–matrix adhesion respectively,  $\gamma$  reflects the degradation rate of matrix by tumour cell-derived proteolytic enzymes and  $n_0$  reflects the effects of crowding on cell proliferation and death, relative to the dimensionless close-packing cell density of 2.

Simultaneously with our work, and independently, Gerisch and Chaplain (2008) have developed a model for cancer invasion that is also based on the work of Armstrong *et al.* (2006). Their model has many similarities to (5), though it differs in a variety of details. To the best of our knowledge, these two models are the first continuum representations of tumour growth to explicitly include the effects of cell–cell and cell–matrix adhesion on cell movement.

To investigate the predictions of the model (5) for tumour growth, we solved the equations numerically for initial conditions corresponding to the introduction of a small, localised tumour cell population into uniform matrix. The resulting behaviour falls into two categories, depending on parameter values. When  $\alpha$  is large compared to  $\beta$ , the tumour cell population increases in the region in which it was introduced, but does not spread out in space (Figure 3). Biologically, this corresponds to a non-invasive tumour developing when cell–cell adhesion dominates cell–matrix adhesion. In the long term, the region occupied by the tumour is simply that in which the cells are initially introduced, and is independent of the initial level of tumour cell density.

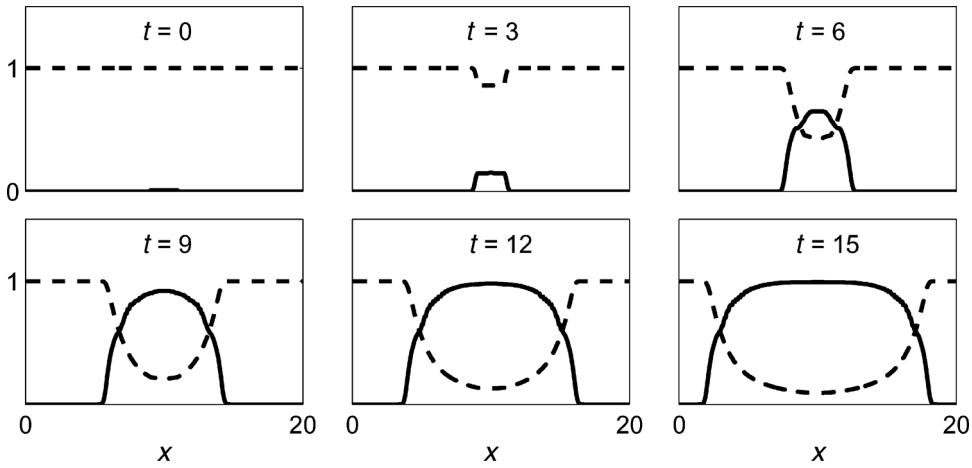


FIGURE 4. Numerical simulation of invasive tumour growth using the model (5). Initially we introduce a small population of tumour cells into a uniform level of extracellular matrix; specifically  $n = 0.01$  on  $9 < x < 11$  and zero elsewhere, and  $m \equiv 1$ , at  $t = 0$ . The parameter values  $\alpha = \gamma = 1$ ,  $\beta = 2$  are such that the tumour invades the surrounding matrix. The function  $\omega(x_0) = \text{sign}(x_0)$ , and the equations were solved numerically as described in the legend to Figure 2. We use zero flux boundary conditions, with the domain sufficiently large that the cell density remains almost zero close to the boundary throughout the solution.

When  $\alpha$  is small compared to  $\beta$ , the small initial population of tumour cells again grows, but also expands, invading the surrounding matrix (Figure 4). Biologically, this corresponds to tumour invasion occurring when cell–matrix adhesion dominates cell–cell adhesion, in keeping with standard thinking about the mechanisms underlying cancer invasion. In Figure 5 we show the division of the  $\alpha$ – $\beta$  parameter plane into invasive and non-invasive cases for one pair of values of the other two parameters  $\gamma$  and  $n_0$ . Calculation of the curve dividing the two types of behaviour in the  $\alpha$ – $\beta$  plane is a natural objective for future work.

#### 4 Mathematical results on boundedness

In our models, the dimensionless cell density of 2 corresponds to close-packing. Therefore, biologically meaningful solutions cannot have cell density increasing through 2, and of course cell density must also be non-negative. We now obtain a number of conditions that are sufficient for these boundedness properties to hold. We formulate our results for the following equation system, which includes both the cell aggregation model (2) and the cancer invasion model (5):

$$\frac{\partial n(x, t)}{\partial t} = D \frac{\partial^2 n}{\partial x^2} - \frac{\partial K}{\partial x} + f(n), \tag{6a}$$

$$\frac{\partial m(x, t)}{\partial t} = -\gamma n m^2, \tag{6b}$$

$$\text{for } t \geq 0, x \in \mathbb{R}$$

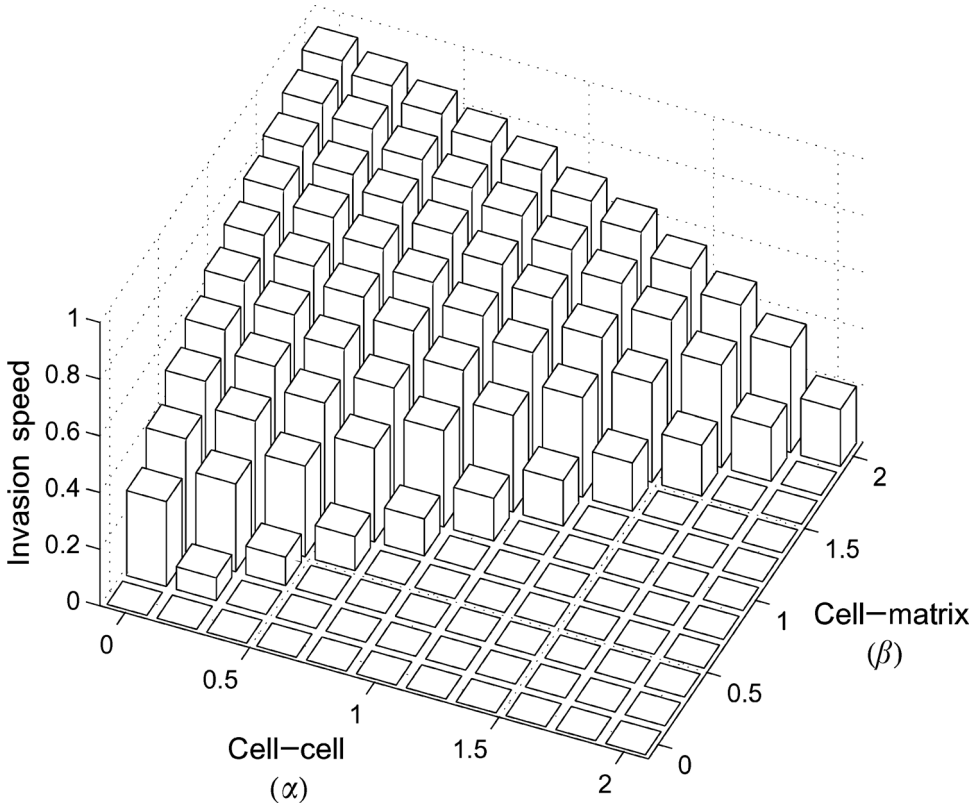


FIGURE 5. A plot of invasion speed as a function of cell-cell adhesion strength,  $\alpha$ , and cell-matrix adhesion strength,  $\beta$ , in the model (5). Speeds of zero correspond to non-invasive tumour growth. The parameter  $\gamma = 1$ . We used initial and boundary conditions as in Figures 3 and 4, and the same method of numerical solution.

$$\text{with } K(x, t) = n(x, t) \int_{-1}^{+1} [ \alpha n(x + x_0, t) + \beta m(x + x_0, t) \cdot g(n(x + x_0, t) + m(x + x_0, t)) \omega(x_0) dx_0 \tag{6c}$$

$$\text{subject to } D \geq 0, \alpha > 0, \beta \geq 0, \gamma \geq 0 \tag{6d}$$

$$\text{and } f(0) = f(n_0) = 0 \text{ for some } n_0 \in (0, 2), \quad f(\xi) > 0 \text{ on } 0 < \xi < n_0, \quad f(\xi) < 0 \text{ on } \xi > n_0 \tag{6e}$$

$$\text{and } g(\xi) > 0 \text{ and bounded on } 0 < \xi < 2, \quad g(\xi) = 0 \text{ on } \xi \geq 2 \tag{6f}$$

$$\text{and } \omega(\cdot) \text{ an odd function, } \omega(\xi) \geq 0 \text{ on } \xi \geq 0, \quad \int_0^1 \omega(x_0) dx_0 = 1. \tag{6g}$$

We will prove the following:

**Proposition 1** *Suppose that  $n(x, t)$  and  $m(x, t)$  satisfy (6) with  $n(x, 0) \geq 0$  and  $m(x, 0) \geq 0$  for all  $x \in \mathbb{R}$ . Then  $n(x, t) \geq 0$  and  $m(x, t) \geq 0$  for all  $t > 0, x \in \mathbb{R}$ .*

**Proposition 2** *Suppose that  $n(x, t)$  and  $m(x, t)$  satisfy (6) with  $0 \leq n(x, 0) \leq 2$  and  $0 \leq m(x, 0) \leq M$  for some  $M > 0$ , for all  $x \in \mathbb{R}$ . Then  $n(x, t) \leq 2$  for all  $t > 0$  and  $x \in \mathbb{R}$  if any of the following conditions hold:*

- (i)  $\omega(x_0) = \text{sign}(x_0)$
- (ii)  $\omega(\cdot)$  is continuous on  $[-1, 1]$  and differentiable on  $(-1, 1)$ , and  $\alpha + \min\{1, \frac{1}{2}M\}\beta < -f(2)[4 \sup\{g(\xi) : 0 < \xi < 2\} \int_{-1}^1 |\omega'(x_0)| dx_0]^{-1}$
- (iii)  $\omega(\cdot)$  is continuous on  $[-1, 1]$  and differentiable on  $(-1, 1)$ , with  $\omega'(x_0) > 0$  on  $|x_0| < x_m$  and  $\omega'(x_0) < 0$  on  $x_m < |x_0| < 1$  for some  $x_m \in (0, 1)$ , and  $\alpha + \min\{1, \frac{1}{2}M\}\beta < -f(2) [8 \sup\{g(\xi) : 0 < \xi < 2\} \omega(x_m)]^{-1}$
- (iv)  $\omega(x_0) = \Omega(\lambda x_0) / \int_0^1 \Omega(\lambda x_0) dx_0$  for  $\lambda > 0$  sufficiently large, where  $\Omega(\cdot)$  is differentiable on  $\mathbb{R}$ ,  $|\Omega'(\eta)| \in L^1(\mathbb{R})$  and  $\Omega(\eta) \rightarrow \pm \Omega^*$  as  $\eta \rightarrow \pm \infty$  for some  $\Omega^* > 0$ , assuming additionally that  $D > 0$  and that there exist  $c > 0$  and  $\epsilon > 0$  such that  $|\partial^3 n / \partial x^3| \leq c \lambda^{3-\epsilon}$  for all  $(x, t) \in \mathbb{R} \times [0, \infty)$

**Remarks** The conditions on  $\omega(\cdot)$  in part (iv) include the normalised  $\tanh(\lambda x_0)$  case which will be discussed later. Note that an  $\omega(x_0)$  satisfying (iv) will tend to the function  $\text{sign}(x_0)$  of case (i), as  $\lambda \rightarrow \infty$ . Thus as  $\lambda \rightarrow \infty$  the model formally becomes independent of  $\lambda$ . This suggests that the solution for case (iv) approaches that for case (i) in this limit, so that the additional assumption on  $|\partial^3 n / \partial x^3|$  for case (iv) is not unrealistic. In fact  $|\partial^3 n / \partial x^3|$  is probably bounded independently of  $\lambda$  as  $\lambda \rightarrow \infty$ , but our proof works even if  $|\partial^3 n / \partial x^3|$  grows with  $\lambda$  to some extent. The restriction  $D > 0$  is required for our proof of case (iv), but we expect the boundedness property to be preserved in the limit  $D \rightarrow 0$ .

Part (iii) of Proposition 2 is included because of its particular importance in the very common situation in which the one-dimensional behaviour represented by (6) actually occurs in a two-dimensional system. In this case,  $n$  and  $m$  will be functions of the cartesian coordinate  $x$  only, independent of  $y$ , but the adhesive flux will be determined by an integral over the two-dimensional sensing region of the cell. Assuming this sensing region to be circular gives

$$K(x, t) = n(x, t) \int_{\theta=0}^{2\pi} \int_{r=0}^1 [xn(x + r \cos \theta, t) + \beta m(x + r \cos \theta, t)] \cdot g(n(x + r \cos \theta, t) + m(x + r \cos \theta, t)) \widehat{\omega}(r) \cos \theta r dr d\theta.$$

Here the positive function  $\widehat{\omega}(\cdot)$  describes the variation in the sensing ability of cells across their sensing region; for simplicity we take this to be a constant. Changing to cartesian coordinates in the integral then gives

$$\begin{aligned} K(x, t) &= n(x, t) \int_{x_0=-1}^1 \int_{y_0=-\sqrt{1-x_0^2}}^{\sqrt{1-x_0^2}} \frac{x_0}{\sqrt{x_0^2 + y_0^2}} [xn(x + x_0, t) + \beta m(x + x_0, t)] \\ &\quad \cdot g(n(x + x_0, t) + m(x + x_0, t)) \widehat{\omega} dy_0 dx_0 \\ &= n(x, t) \int_{-1}^1 [xn(x + x_0, t) + \beta m(x + x_0, t)] \\ &\quad \cdot g(n(x + x_0, t) + m(x + x_0, t)) \widehat{\omega} x_0 \log \left( \frac{1 + \sqrt{1 - x_0^2}}{1 - \sqrt{1 - x_0^2}} \right) dx_0. \end{aligned}$$

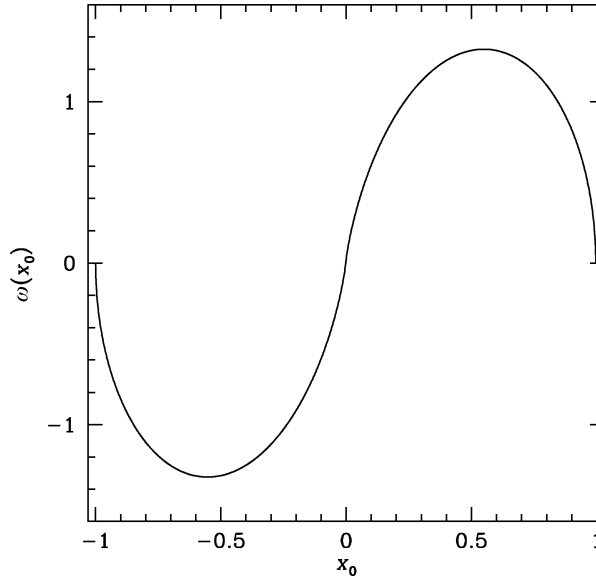


FIGURE 6. A plot of the function  $\omega(x_0)$  given in (7). This is derived by assuming one-dimensional behaviour in a two-dimensional system, with a circular cell sensing region, over which sensing is uniform.

This corresponds to (6c) if we take

$$\omega(x_0) = x_0 \log \left( \frac{1 + \sqrt{1 - x_0^2}}{1 - \sqrt{1 - x_0^2}} \right) \quad (-1 < x_0 < 1); \quad (7)$$

the constant  $\widehat{\omega}$  must be 1 in order to satisfy the integral constraint in (6g). This function, which is illustrated in Figure 6, has the form required for part (iii) of Proposition 2, with  $x_m = 0.552\dots$

**Proof of Proposition 1** Non-negativity of the  $m(x, t)$  variable is clear and is consequent upon the fact that  $m$  satisfies  $m_t = -\gamma n m^2$  which has no spatial derivative terms and in which  $x$  behaves as a parameter. This equation behaves as a one-dimensional ODE in which the right-hand side is zero when  $m = 0$  and for which a local Lipschitz condition holds. Thus  $m(x, t) \geq 0$ .

Now suppose that non-negativity of  $n(x, t)$  ceases to hold at some finite time, considering first the case  $D > 0$ . Then

$$t_{n0} := \sup\{t : n(x, t) \geq 0 \text{ for all } x \in \mathbb{R}\}$$

exists, and there is a point  $x = x_{n0}$  such that  $n(x_{n0}, t_{n0}) = 0$  and  $n(x_{n0}, t_{n0} + 0) < 0$  ( $x_{n0}$  is not necessarily unique). Then at  $(x_{n0}, t_{n0})$ ,

$$n = 0, \quad \frac{\partial n}{\partial x} = 0, \quad \frac{\partial^2 n}{\partial x^2} \geq 0, \quad \frac{\partial n}{\partial t} \leq 0. \quad (8)$$

Note that the second and third terms in the right-hand-side of (6a) are zero at  $(x_{n_0}, t_{n_0})$ . Proof of non-negativity now proceeds by considering separately the two cases  $\partial^2 n(x_{n_0}, t_{n_0})/\partial x^2 > 0$  and  $\partial^2 n(x_{n_0}, t_{n_0})/\partial x^2 = 0$ .

The first case  $\partial^2 n(x_{n_0}, t_{n_0})/\partial x^2 > 0$  is trivial, since evaluating (6a) at  $(x_{n_0}, t_{n_0})$  implies that  $\partial n(x_{n_0}, t_{n_0})/\partial t > 0$ , which contradicts (8). The second case  $\partial^2 n(x_{n_0}, t_{n_0})/\partial x^2 = 0$  is more delicate and implies a higher order of tangency of the graph of  $n(x, t_{n_0})$  to the  $x$ -axis at  $x_{n_0}$ . Unless  $n(x, t_{n_0})$  is zero for all  $x \in \mathbb{R}$  (in which case  $n$  would remain zero for all subsequent  $t$ ), there must exist a spatial derivative of  $n$  of *even* order ( $2i$  say,  $i \in \mathbb{N}$ ) that is *strictly* positive at  $(x_{n_0}, t_{n_0})$ , and with all the lower order spatial derivatives of  $n$  being zero at  $(x_{n_0}, t_{n_0})$ . Then explicit differentiation of (6a) gives

$$\frac{\partial^i n}{\partial t^i} = D^i \frac{\partial^{2i} n}{\partial x^{2i}} > 0$$

at  $(x_{n_0}, t_{n_0})$ , if  $D > 0$ . Since  $n = \partial n/\partial t = \dots = \partial^{i-1} n/\partial t^{i-1} = 0$  at  $(x_{n_0}, t_{n_0})$ , the graph of  $n(x, t)$  must lift off the  $x$ -axis as  $t$  increases from  $t_{n_0}$ , and this contradicts the definition of  $t_{n_0}$ . We have assumed that all relevant derivatives exist. However, for  $D > 0$  this is reasonable because of the well-known smoothing property of the Laplacian operator; see Alibaud *et al.* (submitted) for a detailed discussion of this smoothing property in the context of a (different) non-local equation.

For the case when  $D = 0$ , non-negativity is immediate. Equation (6a) implies that  $\partial n/\partial t = 0$  at  $(x_{n_0}, t_{n_0})$ , and repeated differentiation of this equation with respect to time implies further that  $\partial^i n/\partial t^i = 0$  for all  $i \geq 0$ . Therefore  $n(x_{n_0}, t) = 0$  for all  $t \geq t_{n_0}$ , which contradicts the definition of  $t_{n_0}$ . □

**Proof of Proposition 2** The first stage in the proof is essentially the same for each of the parts (i)–(iv) of the proposition. Suppose that  $n(x, t) \leq 2$  ceases to hold at some finite time. Then

$$t^* := \sup\{t : n(x, t) \leq 2 \text{ for all } x \in \mathbb{R}\}$$

exists;  $n(x, t^*)$  is still  $\leq 2$  everywhere but its graph touches the line  $n = 2$  somewhere. Let  $x^*$  be a value of  $x$  at which such a tangency occurs, with  $n(x^*, t^* + 0) > 2$  ( $x^*$  is not necessarily unique). Then at  $(x^*, t^*)$ ,

$$n = 2, \quad \frac{\partial n}{\partial x} = 0, \quad \frac{\partial^2 n}{\partial x^2} \leq 0, \quad \frac{\partial n}{\partial t} \geq 0 \tag{9}$$

and  $0 \leq n(x, t^*) \leq 2$  for all  $x \in \mathbb{R}$ . Evaluating (6a) at  $(x^*, t^*)$  and making use of (9), we obtain

$$\frac{\partial n}{\partial t} \Big|_{(x^*, t^*)} \leq -2 \frac{\partial}{\partial x} \left( \int_{-1}^1 [ \alpha n(x + x_0, t) + \beta m(x + x_0, t) \right. \\ \left. \cdot g(n(x + x_0, t) + m(x + x_0, t)) \omega(x_0) dx_0 \right) \Big|_{(x^*, t^*)} + f(2)$$

$$\begin{aligned}
 &= -2 \left( \int_{-1}^1 \frac{\partial}{\partial x} \{ [\alpha n(x + x_0, t) + \beta m(x + x_0, t)] \right. \\
 &\quad \left. \cdot g(n(x + x_0, t) + m(x + x_0, t)) \} \omega(x_0) dx_0 \right)_{(x^*, t^*)} + f(2) \\
 &= -2 \left( \int_{-1}^1 \frac{\partial}{\partial x_0} \{ [\alpha n(x^* + x_0, t^*) + \beta m(x^* + x_0, t^*)] \right. \\
 &\quad \left. \cdot g(n(x^* + x_0, t^*) + m(x^* + x_0, t^*)) \} \omega(x_0) dx_0 \right) + f(2). \tag{10}
 \end{aligned}$$

For notational convenience in the following, we define

$$\tilde{g}(x) = [\alpha n(x^* + x, t^*) + \beta m(x^* + x, t^*)]g(n(x^* + x, t^*) + m(x^* + x, t^*)).$$

Considering now part (i) of the proposition, we have  $\omega(x_0) = \text{sign}(x_0)$ , so that the integral on the right-hand side of (10) can be evaluated immediately. This gives

$$\left. \frac{\partial n}{\partial t} \right|_{(x^*, t^*)} \leq -2 [\tilde{g}(1) + \tilde{g}(-1)] + 4\tilde{g}(0) + f(2).$$

Since  $n(x^*, t^*) = 2$  from (9) and  $m(x^*, t^*) \geq 0$  from Proposition 1,  $g(n(x^*, t^*) + m(x^*, t^*)) = 0 \Rightarrow \tilde{g}(0) = 0$ . Therefore

$$\left. \frac{\partial n}{\partial t} \right|_{(x^*, t^*)} \leq -2 [\tilde{g}(1) + \tilde{g}(-1)] \omega(1) + f(2) \leq f(2) < 0.$$

This contradicts (9), which implies part (i) of the proposition.

For parts (ii)–(iv), evaluating the integral in (10) by parts gives

$$\begin{aligned}
 \left. \frac{\partial n}{\partial t} \right|_{(x^*, t^*)} &\leq -2 [\tilde{g}(1) + \tilde{g}(-1)] \omega(1) + 2 \int_{-1}^1 \tilde{g}(x_0) \omega'(x_0) dx_0 + f(2) \\
 &\leq 2I + f(2)
 \end{aligned} \tag{11}$$

where

$$I = \int_{-1}^1 \tilde{g}(x_0) \omega'(x_0) dx_0.$$

To complete the proof, it is sufficient to show that  $2I + f(2) < 0$ , since this then implies that  $\partial n / \partial t < 0$  at  $(x^*, t^*)$ , giving a contradiction with (9).

We will prove that  $2I + f(2) < 0$  is implied by each of the conditions in parts (ii), (iii) and (iv) of the proposition, with case (iv) being considerably more delicate. We begin with part (ii). For all  $x \in \mathbb{R}$ ,  $0 \leq n(x, t^*) \leq 2$ . Moreover, for all  $x \in \mathbb{R}$ , Proposition 1 implies that  $m(x, t^*) \geq 0$ , and equation (6b) implies that  $\partial m / \partial t \leq 0$  for all  $t \geq 0$ , so that  $m(x, t^*) \leq M$ . Therefore

$$\begin{aligned}
 I &\leq \int_{-1}^1 \left| [\alpha n(x^* + x_0, t^*) + \beta m(x^* + x_0, t^*)]g(n(x^* + x_0, t^*) + m(x^* + x_0, t^*)) \omega'(x_0) \right| dx_0 \\
 &\leq \int_{-1}^1 [2\alpha + \min\{M, 2\}\beta] \sup\{g(\xi) : 0 < \xi < 2\} |\omega'(x_0)| dx_0.
 \end{aligned} \tag{12}$$

Here we are using the fact that if  $m(x^* + x_0, t^*) > 2$ , then  $n(x^* + x_0, t^*) + m(x^* + x_0, t^*) > 2$  and thus  $g(n(x^* + x_0, t^*) + m(x^* + x_0, t^*)) = 0$ . Applying the condition in the statement of (ii) then implies that  $2I + f(2) < 0$ , as required.

For part (iii), the argument is very similar:

$$\begin{aligned} I &\leq \int_{-x_m}^{x_m} [\alpha n(x^* + x_0, t^*) + \beta m(x^* + x_0, t^*)] g(n(x^* + x_0, t^*) + m(x^* + x_0, t^*)) \omega'(x_0) dx_0 \\ &\leq \int_{-x_m}^{x_m} [2\alpha + \min\{M, 2\}\beta] \sup\{g(\xi) : 0 < \xi < 2\} \omega'(x_0) dx_0 \\ &= 2[2\alpha + \min\{M, 2\}\beta] \sup\{g(\xi) : 0 < \xi < 2\} \omega(x_m), \end{aligned}$$

and applying the condition in the statement of (iii) then implies that  $2I + f(2) < 0$ , as required.

The proof of part (iv) of the proposition is more delicate. Suppose, for contradiction, that there is a sequence  $\{\lambda_i\}$  of values of  $\lambda$ , with  $\lambda_i \rightarrow \infty$  as  $i \rightarrow \infty$ , for which the variable  $n$  violates the bound  $n(x, t) \leq 2$ . The corresponding values of  $x^*$  and  $t^*$  will depend on  $\lambda_i$  and are therefore denoted as  $x_i^*$  and  $t_i^*$  henceforth. The solution components  $n$  and  $m$  also depend on  $\lambda$ , and we denote them as  $n_i$  and  $m_i$ . At  $(x_i^*, t_i^*)$ ,

$$n_i = 2, \quad \frac{\partial n_i}{\partial x} = 0, \quad \frac{\partial^2 n_i}{\partial x^2} \leq 0, \quad \frac{\partial n_i}{\partial t} \geq 0, \tag{13}$$

with  $0 \leq n_i(x, t_i^*) \leq 2$  for all  $x \in \mathbb{R}$ . The previous parts of the proof are valid up to the point at which we defined the integral hitherto known as  $I$ . In part (iv) the dependence of this integral on  $i$  is important, so it will henceforth be denoted  $I_i$ . Thus

$$I_i = \int_{-1}^1 [\alpha n_i(x_i^* + x_0, t_i^*) + \beta m_i(x_i^* + x_0, t_i^*)] g(n_i(x_i^* + x_0, t_i^*) + m_i(x_i^* + x_0, t_i^*)) \frac{\lambda_i \Omega'(\lambda_i x_0)}{\int_0^1 \Omega(\lambda_i \xi) d\xi} dx_0. \tag{14}$$

It is sufficient to show that  $\limsup_{i \rightarrow \infty} I_i \leq 0$ , since this implies that  $2I_i + f(2)$ , and hence  $\partial n_i(x_i^*, t_i^*)/\partial t$  are negative for sufficiently large  $i$ , which contradicts (13).

It is straightforward to show that

$$\lim_{\lambda \rightarrow \infty} \int_0^1 \Omega(\lambda \xi) d\xi = \Omega^*.$$

(For example, substitute  $\eta = \lambda \xi$  in the integral, and apply l'Hôpital's rule.) Therefore, for sufficiently large  $i$ , the denominator of the integrand in (14) exceeds  $\Omega^*/2$ , so that

$$\begin{aligned} I_i &\leq \frac{2}{\Omega^*} (2\alpha + \beta M) \int_{-1}^1 g(n_i(x_i^* + x_0, t_i^*) + m_i(x_i^* + x_0, t_i^*)) \lambda_i |\Omega'(\lambda_i x_0)| dx_0 \\ &= \frac{2}{\Omega^*} (2\alpha + \beta M) \int_{-\lambda_i}^{\lambda_i} g(n_i(x_i^* + \eta/\lambda_i, t_i^*) + m_i(x_i^* + \eta/\lambda_i, t_i^*)) |\Omega'(\eta)| d\eta \\ &\leq \frac{2}{\Omega^*} (2\alpha + \beta M) \int_{-\infty}^{\infty} g(n_i(x_i^* + \eta/\lambda_i, t_i^*) + m_i(x_i^* + \eta/\lambda_i, t_i^*)) |\Omega'(\eta)| d\eta. \end{aligned}$$

The integrand in the above expression is dominated by

$$\left( \max_{\xi \in [0,2]} g(\xi) \right) |\Omega'(\eta)|$$

which is independent of  $i$  and is in  $L^1(\mathbb{R})$  by hypothesis. This allows us to apply Fatou's lemma, giving

$$\limsup_{i \rightarrow \infty} I_i \leq \frac{2}{\Omega^*} (2\alpha + \beta M) \int_{-\infty}^{\infty} \limsup_{i \rightarrow \infty} g(n_i(x_i^* + \eta/\lambda_i, t_i^*) + m_i(x_i^* + \eta/\lambda_i, t_i^*)) |\Omega'(\eta)| d\eta.$$

We now show that for each fixed  $\eta$ ,

$$\limsup_{i \rightarrow \infty} g(n_i(x_i^* + \eta/\lambda_i, t_i^*) + m_i(x_i^* + \eta/\lambda_i, t_i^*)) = 0.$$

Since  $m_i(\cdot) \geq 0$  and since  $g(\xi) = 0$  when  $\xi \geq 2$ , it is enough to show that  $\lim_{i \rightarrow \infty} n_i(x_i^* + \eta/\lambda_i, t_i^*) = 2$  for each fixed  $\eta$ . This is not completely trivial even though  $n_i(x_i^*, t_i^*) = 2$  for all  $i$ , since  $(x_i^*, t_i^*)$  may not converge as  $i \rightarrow \infty$ . Indeed, due to the unboundedness of the domain in both space and time, it is not even clear if  $(x_i^*, t_i^*)$  has a convergent subsequence in  $\mathbb{R}^2$ . (Otherwise we could have worked with the corresponding subsequence of  $\{\lambda_i\}$  from the outset.) The possible difficulty is to do with the fact that in principle the function  $n_i(\cdot, t_i^*)$  could develop tighter and tighter curvature at  $x_i^*$  as  $i \rightarrow \infty$  such that  $n_i(x_i^* + \eta/\lambda_i, t_i^*)$  stays away from 2, even though  $\eta/\lambda_i \rightarrow 0$ . We will now argue, via a Taylor series expansion and a bound for  $\partial^2 n_i / \partial x^2$  at  $(x_i^*, t_i^*)$ , that this does not in fact happen. Evaluating (6a) at  $(x_i^*, t_i^*)$  and using (13) gives

$$\left. \frac{\partial n_i}{\partial t} \right|_{(x_i^*, t_i^*)} \leq D \left. \frac{\partial^2 n_i}{\partial x^2} \right|_{(x_i^*, t_i^*)} + 2I_i + f(2).$$

This corresponds to (11), except that we have retained the Laplacian term in this case. Therefore

$$\begin{aligned} D \left. \frac{\partial^2 n_i}{\partial x^2} \right|_{(x_i^*, t_i^*)} &\geq \left. \frac{\partial n_i}{\partial t} \right|_{(x_i^*, t_i^*)} - 2I_i - f(2) \\ &\geq -2I_i - f(2) \\ &\geq -\frac{4}{\Omega^*} (2\alpha + \beta M) \left( \max_{\xi \in [0,2]} g(\xi) \right) \int_{-\infty}^{\infty} |\Omega'(\eta)| d\eta - f(2). \end{aligned}$$

Since  $\partial^2 n_i(x_i^*, t_i^*) / \partial x^2 \leq 0$  and  $f(2) < 0$ , it implies that

$$\left| D \left. \frac{\partial^2 n_i}{\partial x^2} \right|_{(x_i^*, t_i^*)} \right| < \frac{4}{\Omega^*} (2\alpha + \beta M) \left( \max_{\xi \in [0,2]} g(\xi) \right) \int_{-\infty}^{\infty} |\Omega'(\eta)| d\eta.$$

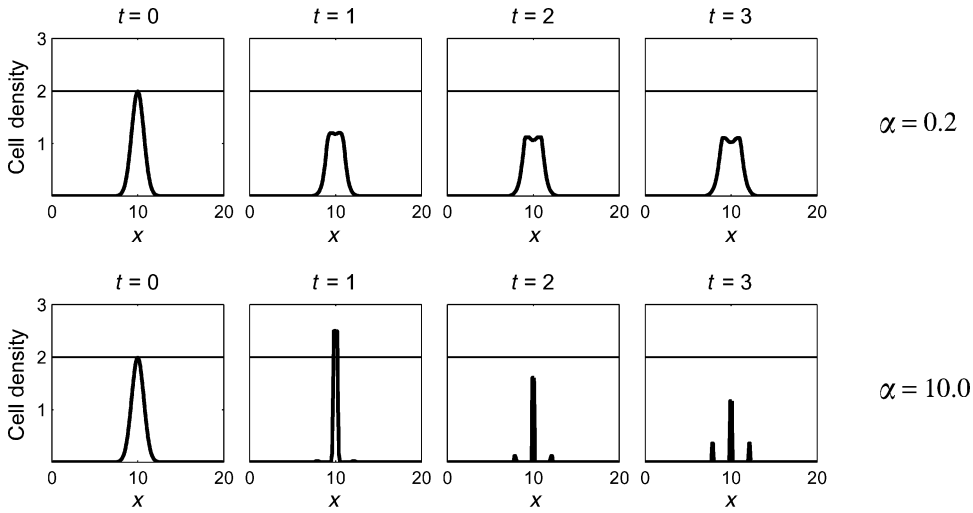


FIGURE 7. Numerical solution of (6) with  $m \equiv 0$ , illustrating the solution for  $n$  remaining below 2 when  $\alpha$  satisfies the condition in Proposition 4(iii), but increasing through 2 (and then decreasing below 2 again) for a larger value of  $\alpha$ . The cell diffusion coefficient  $D=0$ . The functional forms are  $f(n) = n(1 - n)$ ,  $g(n) = \max\{2 - n, 0\}$  and  $\omega(x_0) = x_0 \log[(1 + \sqrt{1 - x_0^2}) / (1 - \sqrt{1 - x_0^2})]$ . The initial condition is  $n(x, 0) = 1.99 \exp[-(x - 10)^2]$  on the domain  $0 \leq x \leq 20$  with zero flux boundary conditions at both ends. For clarity, the line  $n=2$  is superimposed on the solution. The equations were solved numerically as described in the legend to Figure 2.

Then for each fixed  $\eta$  we have, for some  $\theta_i \in (0, 1)$ ,

$$\begin{aligned} |n_i(x_i^* + \eta/\lambda_i, t_i^*) - 2| &= |n_i(x_i^* + \eta/\lambda_i, t_i^*) - n_i(x_i^*, t_i^*)| \\ &= \left| \frac{\eta^2}{2\lambda_i^2} \left[ \frac{\partial^2 n_i}{\partial x^2} \right]_{(x_i^*, t_i^*)} + \frac{\eta^3}{6\lambda_i^3} \left[ \frac{\partial^3 n_i}{\partial x^3} \right]_{(x_i^* + \theta_i \eta/\lambda_i, t_i^*)} \right| \\ &\leq \frac{\eta^2}{2D\lambda_i^2} \left[ \frac{4}{\Omega^*} (2\alpha + \beta M) \left( \max_{\xi \in [0, 2]} g(\xi) \right) \int_{-\infty}^{\infty} |\Omega'(\eta)| d\eta \right] + \frac{c|\eta|^3}{6\lambda_i^\epsilon} \end{aligned}$$

for  $i$  sufficiently large, where we have used  $|\partial^3 n_i / \partial x^3| \leq c\lambda_i^{3-\epsilon}$ . (Recall that we assume  $D > 0$  for this part of the proposition.) Therefore, for each fixed  $\eta$ ,  $\lim_{i \rightarrow \infty} n_i(x_i^* + \eta/\lambda_i, t_i^*) = 2$ , which is what we needed to show. We now have that  $\limsup_{i \rightarrow \infty} I_i \leq 0$  which, as explained previously, leads to  $\partial n_i(x_i^*, t_i^*) / \partial t < 0$  for sufficiently large  $i$ , which contradicts (13).  $\square$

**Numerical investigation of boundedness** Numerical simulations suggest that when the conditions in Proposition 2 do not hold, the solution for  $n$  may increase through 2. In Figures 7 and 8 we show two examples of this. In both cases, we fix  $m \equiv 0$  (implying that we can choose  $M = 0$ ) and take  $f(n) = n(1 - n)$  and  $g(n) = \max\{2 - n, 0\}$ . In the first case, we use the form of  $\omega(\cdot)$  given in (7). Part (iii) of Proposition 2 then implies that the solution for  $n$  remains less than 2 when  $\alpha < 0.377\dots$ : note that this condition is sufficient but not necessary. Figure 7 illustrates solutions in which  $n$  increases through 2 for  $\alpha$  above this critical value, but remains less than 2, for the same initial conditions, when  $\alpha$

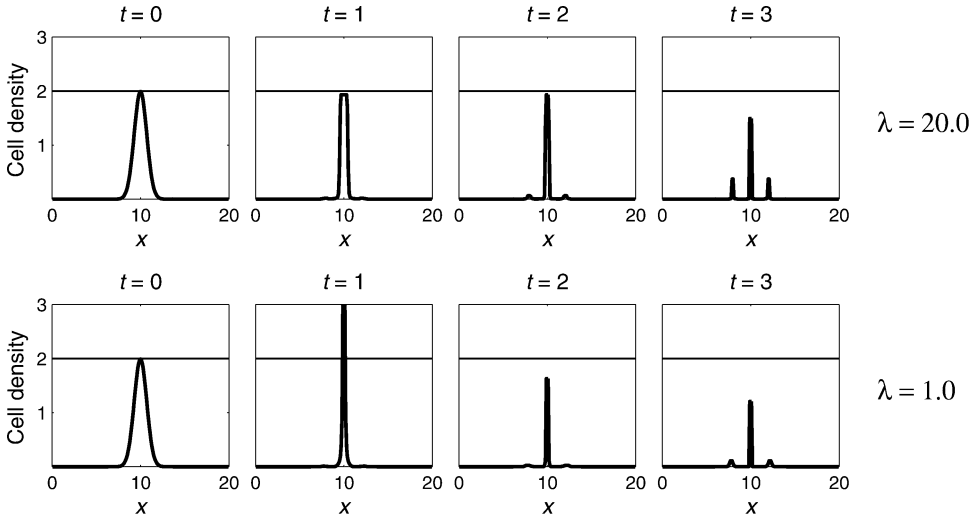


FIGURE 8. Numerical solution of (6) with  $m \equiv 0$  and with  $\omega(\cdot)$  having a form corresponding to part (iv) of Proposition 2. The solution for  $n$  remains below 2 when  $\lambda$  is large, but increases through 2 (and then decreases below 2 again) for a smaller value of  $\lambda$ . The adhesion coefficient  $\alpha = 5$ , and the cell diffusion coefficient  $D = 0.0001$ . The functional forms are  $f(n) = n(1 - n)$ ,  $g(n) = \max\{(2 - n), 0\}$  and  $\omega(x_0) = \tanh(\lambda x_0) \cdot \lambda / \log \cosh \lambda$ . The initial condition is  $n(x, 0) = 1.99 \exp[-(x - 10)^2]$  on the domain  $0 \leq x \leq 20$ , with zero flux boundary conditions at both ends. For clarity, the line  $n = 2$  is superimposed on the solution. The equations were solved numerically as described in the legend to Figure 2. For this figure, we have deliberately used a very small value of  $D$ ; the corresponding solutions with  $D = 0$  are indistinguishable from those shown. This reinforces our comment after the statement of Proposition 2 that we expect boundedness to be preserved in the limit as  $D \rightarrow 0$ .

is smaller. In Figure 8 we use  $\omega(x_0) = Q(\lambda) \tanh(\lambda x_0)$ , where  $Q(\lambda)$  is chosen to satisfy the integral constraint in (6g) (specifically  $Q(\lambda) = \lambda / \log \cosh \lambda$ ). Part (iv) of Proposition 2 then implies that the solution for  $n$  remains less than 2 provided that  $\lambda$  is sufficiently large. The figure illustrates a solution in which  $n$  increases through 2 for  $\lambda = 1$ , but remains less than 2, for the same initial conditions, when  $\lambda$  is larger.

## 5 Discussion

Previously, Armstrong *et al.* (2006) demonstrated aggregation patterns in numerical simulations of their model for cell adhesion. In this paper, we have extended these results to an expanded version of their model including cell proliferation, showing that the level of intercellular adhesion required for aggregation goes up as the proliferation rate is increased. Furthermore, we have used the representation of adhesion by Armstrong *et al.* (2006) in a new model for cancer invasion, demonstrating a requirement for cell–matrix adhesion to dominate cell–cell adhesion in an invasive phenotype. These successful applications of the model, combined with other recent applications to developmental biology (Armstrong *et al.*, in press) and cancer (Gerisch & Chaplain, 2008), and very similar modelling of liver cell aggregation (Green *et al.*, in preparation), mean that it is important to put the model on a firm mathematical footing. In particular, there is a need to investigate

when the solutions for cell density remain within the bounds demanded by biological realism, namely zero (lower bound) and the density corresponding to close cell packing (upper bound). We have proved the first results of this type, showing that the positivity requirement is satisfied for a broad class of functional forms in the model and deriving a number of conditions, each of which is sufficient for the upper bound to hold. This is the first step in the study of boundedness for the model, and we now summarise what we see as the main outstanding questions.

1. When the adhesion coefficients  $\alpha$  and  $\beta$  are zero, standard theory for reaction–diffusion equations implies that the boundedness conditions always hold for (6). Therefore, for any given functions  $f$ ,  $g$ ,  $\omega$  and parameters  $D$ ,  $\gamma$ , the conditions either hold for all  $\alpha, \beta \geq 0$ , or fail as  $\alpha$  is increased through some critical curve in the  $\alpha$ – $\beta$  plane. Our Proposition 2 shows that the former applies in two cases (parts (i) and (iv)) and the latter in the other two cases (parts (ii) and (iii)) and gives upper bounds on the critical values of  $\alpha$  and  $\beta$ . The key outstanding issue is to extend these results in the direction of a comprehensive classification for general functions and parameters, with a precise form for the critical curve determining boundedness in the  $\alpha$ – $\beta$  plane.
2. Armstrong *et al.* (2006) consider aggregation patterns for (2) when  $f \equiv 0$ , a possibility excluded by (6e). Although almost all cell populations do undergo division, it can be very slow in comparison to the rates of cell movement and rearrangement, so that there can be no cell division at all on the time scale of some *in vitro* experiments. Therefore, investigation of boundedness when  $f \equiv 0$  is important. The numerical simulations of Armstrong *et al.* (2006) suggest that the required boundedness conditions continue to hold for many  $\alpha$  and  $\omega(\cdot)$ ; however, analytical work is significantly more difficult in this case.
3. Armstrong *et al.* (2006) discuss two extensions to their model for cell aggregation, both of which are important biologically but which lack any boundedness results at present. The first is two interacting cell populations, without any term for adhesion to extracellular matrix. This gives a model consisting of two coupled integro-PDES with three adhesion parameters: self-adhesion for each cell population and cross-adhesion between the populations. In this case the boundedness requirements apply to the sum of the two cell densities, and derivation of corresponding constraints on the three adhesion parameters is a major mathematical challenge. The second extension is to higher space dimensions. Most solid tumour growth occurs in three dimensions, while some developmental processes and many *in vitro* experiments are effectively two-dimensional. In higher dimensions, the non-local term in the model involves a multiple integral, and derivation of conditions for boundedness will be significantly more difficult than in one dimension.

### Acknowledgements

NJA was supported by a Doctoral Training Account Studentship from EPSRC. KJP and JAS were supported in part by Integrative Cancer Biology Program Grant CA113004 from the US National Institutes of Health and in part by BBSRC and EPSRC funding to the Centre for Systems Biology at Edinburgh.

## References

- ALA-AHO, R. & KÄHÄRI, V.-M. (2005) Collagenases in cancer. *Biochimie* **87**, 273–286.
- ALBERTS, B., JOHNSON, A., LEWIS, J., RAFF, M., ROBERTS, K. & WALTER, P. (2008) *The Molecular Biology of the Cell, 5th ed.*. Garland Science, New York.
- ALIBAUD, N., AZÉRAD, P. & ISÈBE, D. (submitted) A non-monotone non-local conservation law for dune morphodynamics.
- ANDERSON, A. R. A. (2005) A hybrid mathematical model of solid tumour invasion: The importance of cell adhesion. *IMA J. Math. Appl. Med. Biol.* **22**, 163–186.
- ANDERSON, A. R. A., CHAPLAIN, M. A. J. & REJNIAK, K. A. (eds.) (2007) *Single-Cell-Based Models in Biology and Medicine*. Birkhäuser, Basel.
- ANDERSON, A. R. A., WEAVER, A. M., CUMMINGS, P. T. & QUARANTA, V. (2006) Tumor morphology and phenotypic evolution driven by selective pressure from the microenvironment. *Cell* **127**, 905–915.
- ARAUJO, R. & MCELWAIN, L. (2004) A history of the study of solid tumour growth: The contribution of mathematical modelling. *Bull. Math. Biol.* **66**, 1039–1091.
- ARMSTRONG, N. J., PAINTER, K. J. & SHERRATT, J. A. (2006) A continuum approach to modelling cell–cell adhesion. *J. Theor. Biol.* **243**, 98–113.
- ARMSTRONG, N. J., PAINTER, K. J. & SHERRATT, J. A. (in press) Adding adhesion to the cell cycle model for somite formation. *Bull. Math. Biol.*
- BAUER, A. L., JACKSON, T. L. & JIANG, Y. (2007) A cell-based model exhibiting branching and anastomosis during tumor-induced angiogenesis. *Biophys. J.* **92**, 3105–3121.
- BERRIER, A. L. & YAMADA, K. M. (2007) Cell–matrix adhesion. *J. Cell. Physiol.* **213**, 565–573.
- BYRNE, H. M. (1997) The importance of intercellular adhesion in the development of carcinomas. *IMA J. Math. Appl. Med. Biol.* **14**, 305–323.
- BYRNE, H. M. & CHAPLAIN, M. A. J. (1996) Modelling the role of cell–cell adhesion in the growth and development of carcinomas. *Math. Comp. Modelling* **24**(12), 1–17.
- CHAPLAIN, M. A. J. (1996) Avascular growth, angiogenesis and vascular growth in solid tumours: The mathematical modelling of the stages of tumour development. *Math. Comp. Modelling* **23**(6), 47–87.
- CHAPLAIN, M. A. J. & LOLAS, G. (2005) Mathematical modelling of cancer cell invasion of tissue: The role of the urokinase plasminogen activation system. *Math. Models Methods Appl. Sci.* **15**, 1685–1734.
- CHENG, X., DEN, Z. N. & KOCH, P. J. (2005) Desmosomal cell adhesion in mammalian development. *Eur. J. Cell Biol.* **84**, 215–223.
- CRISTINI, V., LOWENGRUB, J. & NIE, Q. (2003) Nonlinear simulation of tumour growth. *J. Math. Biol.* **46**, 191–224.
- DALLON, J. C. & OTHMER, H. G. (2004) How cellular movement determines the collective force generated by the *Dictyostelium discoideum* slug. *J. Theor. Biol.* **231**, 203–222.
- DEUTSCH, A. & DORMANN, S. (2005) *Cellular Automaton Modeling of Biological Pattern Formation: Characterization, Applications, and Analysis*. Birkhäuser, Boston.
- DRASDO, D. & FORGACS, G. (2000) Modeling the interplay of generic and genetic mechanisms in cleavage, blastulation, and gastrulation. *Dev. Dyn.* **219**, 182–191.
- DRASDO, D. & HOHME, S. (2003) Individual-based approaches to birth and death in avascular tumors. *Math. Comp. Modelling* **37**(11), 1163–1175.
- DRASDO, D. & HOHME, S. (2005) A single-cell-based model of tumor growth *in vitro*: Monolayers and spheroids. *Phys. Biol.* **2**, 133–147.
- DRASDO, D., KREE, R. & MCCASKILL, J. S. (1995) Monte-Carlo approach to tissue–cell populations. *Phys. Rev. E* **52**, 6635–6657.
- DRASDO, D. & LOEFFLER, M. (2001) Individual-based models to growth and folding in one-layered tissues: Intestinal crypts and early development. *Nonlinear Anal.* **47**, 245–256.

- FOGELSON, A. L. (2007) Cell-based models of blood clotting. In: A. R. A. Anderson, M. A. J. Chaplain & K. A. Rejniak (editors), *Single-Cell-Based Models in Biology and Medicine*, Birkhäuser, Basel, pp. 243–269.
- FOGELSON, A. L. & GUY, R. D. (2008) Immersed-boundary-type models of intravascular platelet aggregation. *Comput. Methods Appl. Mech. Engng.* **197**, 2087–2104.
- FOTY, R. A. & STEINBERG, M. S. (2004) Cadherin-mediated cell–cell adhesion and tissue segregation in relation to malignancy. *Int. J. Dev. Biol.* **48**, 397–409.
- FOTY, R. A. & STEINBERG, M. S. (2005) The differential adhesion hypothesis: A direct evaluation. *Dev. Biol.* **278**, 255–263.
- FRIEBOES, H. B., LOWENGRUB, J. S., WISE, S., ZHENG, X., MACKLIN, P., ELAINE, L. B. D. & CRISTINI, V. (2007) Computer simulation of glioma growth and morphology. *Neuroimage* **37**(Suppl. 1), S59–S70.
- FRIEBOES, H. B., ZHENG, X., SUN, C.-H. & TROMBERG, B. (2006) An integrated computational/experimental model of tumour invasion. *Cancer Res.* **66**, 1597–1604.
- FRIEDMAN, A. (2007) Mathematical analysis and challenges arising from models of tumor growth. *Math. Models Methods Appl. Sci.* **17**, 1751–1772.
- GALLE, J., AUST, G., SCHALLER, G., BEYER, T. & DRASDO, D. (2006) Individual cell-based models of the spatial-temporal organization of multicellular systems – Achievements and limitations. *Cytometry* **69A**, 704–710.
- GALLE, J., LOEFFLER, M. & DRASDO, D. (2005) Modelling the effect of deregulated proliferation and apoptosis on the growth dynamics of epithelial cell populations *in vitro*. *Biophys. J.* **88**, 62–75.
- GASSMANN, P., ENNS, A. & HAIER, J. (2004) Role of tumor cell adhesion and migration in organ-specific metastasis formation. *Onkologie* **27**, 577–582.
- GERISCH, A. (submitted) On the approximation and efficient evaluation of integral terms in PDE models of cell adhesion.
- GERISCH, A. & CHAPLAIN, M. A. J. (2008) Mathematical modelling of cancer cell invasion of tissue: Local and non-local models and the effect of adhesion. *J. Theor. Biol.* **250**, 684–704.
- GLAZIER, J. A. & GRANER, F. (1993) Simulation of the differential adhesion driven rearrangement of biological cells. *Phys. Rev. E* **47**, 2128–2154.
- GLAZIER, J. A., RAPHAEL, R. C., GRANER, F. & SAWADA, Y. (1995) The energetics of cell sorting in three dimensions. In: D. Beysens, G. Forgacs & F. Gaill (editors), *Interplay of Genetic and Physical Processes in the Development of Biological Form*, World Scientific Publishing Company, Singapore, pp. 54–61.
- GRANER, F. & GLAZIER, J. A. (1992) Simulation of biological cell sorting using a two-dimensional extended Potts model. *Phys. Rev. Lett.* **69**, 2013–2016.
- GREEN, J. E. F., WATERS, S. L., SHAKESHEFF, K. M., EDELSTEIN-KESHET, L. & BYRNE, H. M. (in preparation) Non-local models for the interactions of hepatocytes and stellate cells during aggregation.
- GRYGIERZEC, W., DEUTSCH, A., PHILIPSEN, L., FRIEDENBERGER, M. & SCHUBERT, W. (2004) Modelling tumour cell population dynamics based on molecular adhesion assumptions. *J. Biol. Syst.* **12**, 273–288.
- HALBLEIB, J. M. & NELSON, W. J. (2006) Cadherins in development: Cell adhesion, sorting, and tissue morphogenesis. *Genes Dev.* **20**, 3199–3214.
- HART, I. (2005) The spread of tumours. In: M. Knowles & P. Selby (editors), *Introduction to the Cellular and Molecular Biology of Cancer*, Oxford University Press, Oxford, UK, pp. 278–288.
- HILLEN, T. & PAINTER, K. J. (2008) A users guide to PDE models for chemotaxis. *J. Math. Biol.* **58**, 183–217.
- JORGENSEN, P. & TYERS, M. (2004) How cells coordinate growth and division. *Curr. Biol.* **14**, R1014–R1027.
- KIM, Y., STOLARSKA, M. & OTHMER, H. G. (2007) A hybrid model for tumor spheroid growth *in vitro* I: Theoretical development and early results. *Math. Models Methods Appl. Sci.* **17**, 1773–1798.

- LOCK, J. G., WEHRLE-HALLER, B. & STROMBLAD, S. (2008) Cell–matrix adhesion complexes: Master control machinery of cell migration. *Seminars Cancer Biol.* **18**, 65–76.
- MACKLIN, P. & LOWENGRUB, J. (2007) Nonlinear simulation of the effect of microenvironment on tumor growth. *J. Theor. Biol.* **245**, 677–704. See also the *erratum* on p. 581 of vol. 247.
- MAREE, A. F. & HOGEWEG, P. (2002) Modelling *Dictyostelium discoideum* morphogenesis: The culmination. *Bull. Math. Biol.* **64**, 327–353.
- MERKS, R. M. H. & GLAZIER, J. A. (2005) A cell-centered approach to developmental biology. *Physica A* **352**, 113–130.
- MOMBACH, J. C. M., GLAZIER, J. A., RAPHAEL, R. C. & ZAJAC, M. (1995) Quantitative comparison between differential adhesion models and cell sorting in the presence and absence of fluctuations. *Phys. Rev. Lett.* **75**, 2244–2247.
- MOREIRA, J. & DEUTSCH, A. (2005) Pigment pattern formation in zebrafish during late larval stages: A model based on local interactions. *Dev. Dyn.* **232**, 33–42.
- PALSSON, E. (2007) A 3-D deformable ellipsoidal cell model with cell adhesion and signalling. In: A. R. A. Anderson, M. A. J. Chaplain & K. A. Rejniak (editors), *Single-Cell-Based Models in Biology and Medicine*, Birkhäuser, Basel, pp. 271–299.
- PALSSON, E. & OTHMER, H. G. (2000) A model for individual and collective cell movement in *Dictyostelium discoideum*. *Proc. Natl. Acad. Sci. USA* **97**, 10448–10453.
- PERUMPANANI, A. J., SHERRATT, J. A., NORBURY, J. & BYRNE, H. M. (1996) Biological inferences from a mathematical model for malignant invasion. *Invasion Metastasis* **16**, 209–221.
- REDDIG, P. J. & JULIANO, R. L. (2005) Clinging to life: Cell to matrix adhesion and cell survival. *Cancer Metastasis Rev.* **24** 425–439.
- SAVILL, N. J. & HOGEWEG, P. (1997) Modelling morphogenesis: From single cells to crawling slugs. *J. Theor. Biol.* **184**, 229–235.
- SAVILL, N. J. & SHERRATT, J. A. (2003) Control of epidermal stem cell clusters by Notch-mediated lateral induction. *Dev. Biol.* **258**, 141–153.
- SCHALLER, G. & MEYER-HERMANN, M. (2007) A modelling approach towards epidermal homeostasis control. *J. Theor. Biol.* **247**, 554–573.
- STEINBERG, M. S. (1962) On the mechanism of tissue reconstruction by dissociated cells, III. Free energy relations and the reorganization of fused, heteronomic tissue fragments. *Proc. Natl. Acad. Sci. USA* **48**, 1769–1776.
- STEINBERG, M. S. (2007) Differential adhesion in morphogenesis: A modern view. *Curr. Op. Genetics Dev.* **17**, 281–286.
- STOTT, E. L., BRITTON, N. F., GLAZIER, J. A. & ZAJAC, M. (1999) Stochastic simulation of benign avascular tumour growth using the Potts model. *Math. Comp. Modelling* **30**(5–6), 183–198.
- TURNER, S. & SHERRATT, J. A. (2002) Intercellular adhesion and cancer invasion: A discrete simulation using the extended Potts model. *J. Theor. Biol.* **216**, 85–100.
- TURNER, S., SHERRATT, J. A. & CAMERON, D. (2004) Tamoxifen treatment failure in cancer and the nonlinear dynamics of TGF $\beta$ . *J. Theor. Biol.* **229**, 101–111.
- WEINER, R., SCHMITT, B. & PODHAISKY, H. (1997) Rowmap – A row-code with Krylov techniques for large stiff odes. *Appl. Num. Math.* **25**, 303–319.
- ZAJAC, M., JONES, G. L. & GLAZIER, J. A. (2000) Model of convergent extension in animal morphogenesis. *Phys. Rev. Lett.* **85**, 2022–2025.
- ZIGRINO, P., LÖFFEK, S. & MAUCH, C. (2005) Tumor-stroma interactions: Their role in the control of tumor cell invasion. *Biochimie* **87**, 321–328.